LETTERS
PUBLISHED ONLINE: 25 OCTOBER 2009 | DOI: 10.1038/NPHOTON.2009.190
nature photonics

Exciton-lattice polaritons in multiple-quantum-well-based photonic crystals

David Goldberg[1], Lev I. Deych[1], Alexander A. Lisyansky[1], Zhou Shi[1], Vinod M. Menon[1]*, Vadim Tokranov[2], Michael Yakimov[2] and Serge Oktyabrsky[2]

Coherent interaction of an ensemble of dipole active atoms or excitons with a vacuum electromagnetic field has been studied extensively since its initial conception by Dicke in 1954[1–6]. However, when the emitters are not only periodically arranged as in refs 2 to 4, but are also placed in a periodically modulated dielectric environment, the interaction between them is carried by the electromagnetic Bloch waves of the photonic crystal[7,8]. Here we report the first observation of this effect using a periodic arrangement of GaAs/AlGaAs quantum wells. The formation of coherently coupled photonic-crystal excitonic-lattice polaritons manifests in our experiments through enhanced reflectivity and reconstruction of the photonic bandgap in the vicinity of the excitons. Experimental evidence of hybrid light hole–heavy hole excitonic-lattice polaritons is also presented. Coherent coupling between excitons and Bloch waves is established through comparisons of the experimental results with theory. Finally, we demonstrate the tuning of these polariton states by an electric field.

Modification of the optical properties of emitters by confining their electromagnetic field in structures such as microcavities and photonic crystals have been studied extensively. Another method of manipulation of optical properties is based on the possibility of coherent radiative coupling between a collection of emissive species. R. H. Dicke showed[1] that if the spacing between the emitters was much smaller than their emission wavelength, the emitters became coherently coupled by the common radiative field. As a result, new collective states are formed, with one of them exhibiting the effect of superradiance. A similar phenomenon can also be realized when the emitters are arranged periodically in a uniform dielectric background or vacuum with the period equal to half of the emission wavelength[2]. In this geometry, the radiative enhancement is due to the Bragg resonance and has been observed in optical lattices of cold atoms[9] and their semiconductor analogue—Bragg multiple quantum well (MQW) structures with negligible dielectric contrast[4]. If the number of periods of such a structure exceeds a certain value, the character of the light–matter interaction further changes, transforming the super-radiant mode into a photonic bandgap[7,10]. More recently, similar effects have been observed in quasi-periodic structures[11].

In the case of Bragg MQW structures, the interaction between the excitons and their emitted photons forms hybrid excitations, called exciton-lattice polaritons (ELPs). If vacuum photons are replaced with Bloch modes of a photonic crystal as mediators of radiative coupling between excitons, the properties of the resulting Bloch-exciton-lattice polaritons (Bloch-ELPs) will significantly change. The combination of the photonic crystal effect with the ELP effect provides two powerful tools to control the light–matter interaction. Similar control can be implemented in other systems such as a atomic lattice and organic materials, in which coherently coupled emissive species can be made to interact with an underlying photonic crystal. Although theoretical considerations of such systems have been explored in detail[12–17], much less experimental work has been carried out in this context[8,18]. In the presence of two excitonic species (heavy hole and light hole excitons in our case), the radiation may coherently couple to both of them, producing exotic hybrid polariton states that have contributions from two material excitations and the photon. The hybrid and collective nature of these polariton states, together with their dispersive properties, make them attractive for slow-light enhanced nonlinear optical applications and for studying macroscopic coherence in solid-state systems[16,19–23].

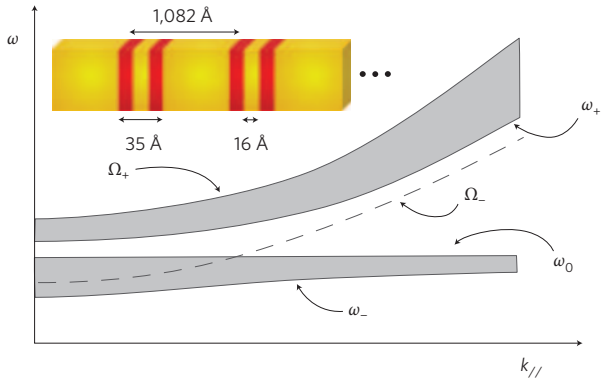

Figure 1 | Dispersion schematic. Dispersion diagram for a Bragg multiple quantum well (MQW) structure when the excitonic frequency ω_0 lies between the two photonic crystal band edges (Ω_+ and Ω_-) at normal incidence. The coherent interaction between the excitons and the photonic crystal Bloch modes results in a modified photonic band structure consisting of two bandgaps, the lower frequency band edges (ω_+ and ω_-) of which anti-cross. The inset shows a schematic of the Bragg MQW structure used in the present study. The structure consists of 70 periods of a double quantum well (DQW) basis with 35 Å thick GaAs quantum wells separated by a 16 Å $Al_{0.22}Ga_{0.78}As$ barrier. A 996 Å $Al_{0.22}Ga_{0.78}As$ barrier separates each pair of the DQWs, resulting in a structure with a period of 1,082 Å.

In this paper we present the first experimental observation of coherent interaction between two excitonic lattices and a photonic crystal. Interaction between the photonic crystal and a single excitonic lattice manifests itself as a combination of two effects: (i) anti-crossing of the exciton mode and the lower frequency band edge mode of the photonic crystal and (ii) the formation of an enhanced photonic-crystal polariton bandgap with a propagation band[12,13,15], as shown schematically in Fig. 1. In the presence of a second excitonic resonance, the interaction is further modified,

[1]Department of Physics, Queens College of the City University of New York (CUNY) Flushing, New York 11367, USA, [2]College of Nanoscience and Engineering, University at Albany, SUNY, 255 Fuller Road, Albany, New York 12203, USA. *e-mail: vinod.menon@qc.cuny.edu

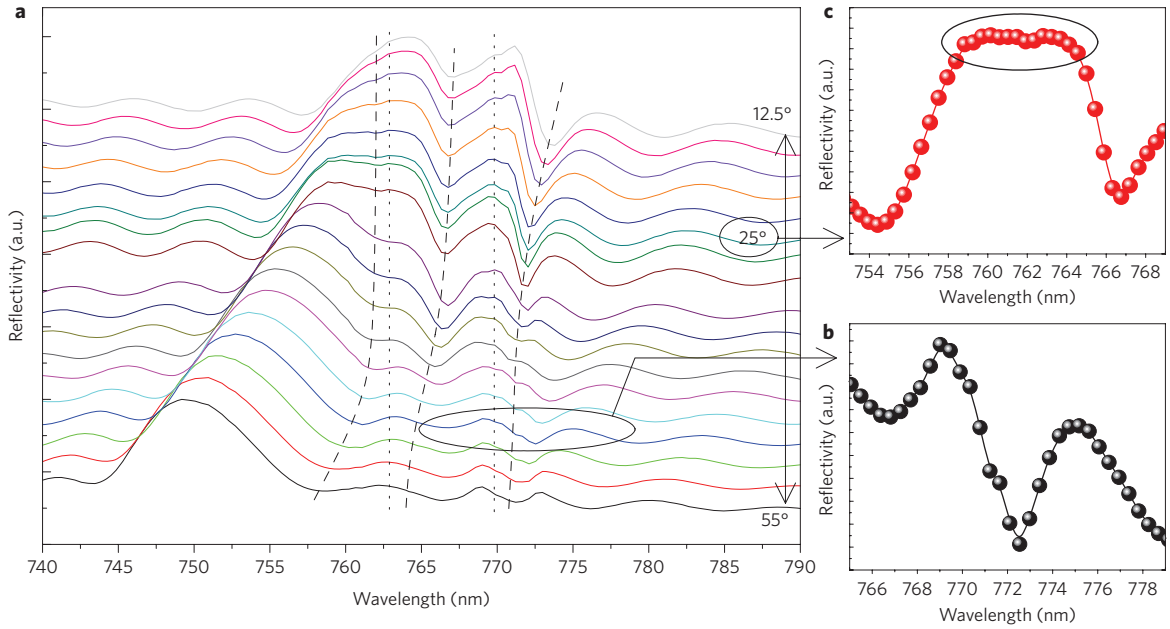

Figure 2 | Angle-dependent reflectivity. a, Reflectivity for an angle of incidence varying from 12.5° (top curve), in increments of 2.5°, up to 55° (bottom curve). The two vertical dotted lines indicate the spectral position of the two excitons and the three dashed lines identify the coupled exciton-lattice polariton features that appear as dips in reflectivity. **b**,**c**, Expanded views showing two notable spectral features in reflectivity: a Fano-like asymmetric spectral feature observed at the hh-exciton frequency when the Bragg peak is sufficiently detuned (**b**); formation of a Bloch-lh-ELP bandgap at 25° with the gap having a flatter top and steeper edges (**c**). In addition, there is a shallow dip present in the middle of the bandgap (**c**) that is characteristic of the coherent interaction between the excitons and the photonic crystal Bloch modes.

resulting in a second anti-crossing between this excitonic mode and the modified low-frequency band edge. This results in the formation of an even larger hybrid bandgap with a second propagating mode. Experimentally, this is demonstrated using angle-dependent reflectivity measurements carried out on a 70-period GaAs/$Al_{0.22}Ga_{0.78}As$ MQW structure with a refractive index difference of 0.22. A schematic of the structure is shown as an inset to Fig. 1. Details of the investigated structure are discussed in the Methods section. The period of the structure is such that the excitonic lattice formed by light-hole (lh) excitons is in the proximity of the bandgap of the photonic crystal. The modification of reflectivity, however, was also observed in the vicinity of heavy-hole (hh) excitons. These observations are interpreted in terms of coherent coupling between the excitonic lattice of the MQW and photonic crystal and formation of hybrid Bloch-lh-hh-ELPs. The experimental results are complemented by theoretical modelling of the structure under investigation using a coupled oscillator model[24] and the more rigorous formalism developed in refs 14 and 25.

The results of angle-dependent reflectivity measurements at 10 K are shown in Fig. 2a. For large angles, where the excitons are detuned from the Bragg peak, a small exciton-related feature consisting of a peak and a dip is visible in the vicinity of the frequency of the hh-exciton, as shown in Fig. 2b. The excitonic nature of this feature at large angles (>40°) is confirmed by its Fano-like asymmetric shape, which is characteristic of electromagnetic Bloch modes scattering off excitons. We do not observe a similar feature at the position of the lh-exciton, which can be explained by its smaller oscillator strength. However, we do see a significant increase in the reflectivity accompanied by a change in the shape of the reflection band when the photonic-crystal bandgap moves closer to the lh-excitonic frequency. At 25° we observe the modified bandgap formed by the Bloch-lh-ELPs. This bandgap is much flatter, wider, and has steeper edges compared to a pure photonic-crystal bandgap (Fig. 2c), and has a shallow dip inside it. This dip, which can be clearly seen, despite being smeared by the non-radiative linewidth of excitons, is a manifestation of the Bloch-lh-ELPs. At even smaller angles, the low-frequency band edge of this modified bandgap interacts with the hh-excitons, resulting in a strong enhancement in reflection in its spectral vicinity, forming a hybrid Bloch-lh-hh-ELP bandgap. For angles between 12.5° and 27.5° another, much more pronounced dip between the lh- and hh-exciton frequencies is observed. It has a slow dispersion, indicative of the photon-lh-hh-exciton hybrid composition of this state. The dispersion of the band edge features observed in angle-dependent reflectivity measurements along with theoretical fits obtained using a coupled oscillator model[24] are shown in Fig. 3a. Three polariton branches, accompanied by two anti-crossings, are observed, with the first anti-crossing occurring at ∼45° between the long-wavelength edge of the photonic-crystal bandgap and the lh-exciton. The second anti-crossing is observed at ∼25° in the vicinity of the hh-exciton. The estimated strengths for the interaction between the excitons and the photons are 4.3 meV and 6.2 meV for the lh- and hh-excitons, respectively.

We calculated the contributions from the lh, hh and photonic components by fitting the experimentally observed dispersion to a three coupled oscillator model, as shown in Fig. 3b. The central polariton branch in the dispersion diagram can be interpreted as having contributions from all three components, and the upper and lower polariton branches have contributions primarily from the photons and one of the excitonic species. At 35°, the central polariton branch has an ∼30% contribution from each of the excitonic species and 40% from the photons. This demonstrates the formation of a hybrid Bloch-lh-hh-ELP.

In addition to the simpler coupled oscillator model, we have also calculated the dispersion characteristics of the polariton branches using the rigorous theoretical model developed in refs 14 and 25 (see Methods section). The results of these calculations, together with the experimental dispersion, are shown in Fig. 4. At large angles, when the photonic crystal bandgap is significantly detuned from the excitonic resonances, the band edges follow the expected

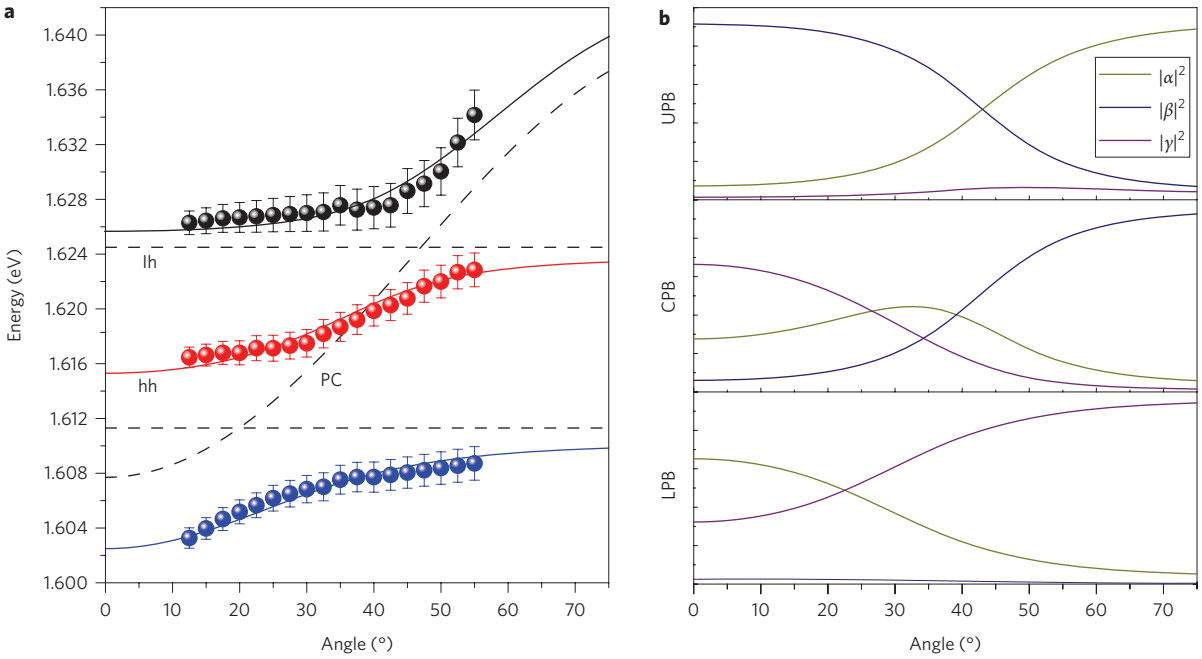

Figure 3 | Polariton dispersion. a, Resonant dips observed in reflectivity plotted as a function of angle indicate the presence of three polariton branches exhibiting characteristic anti-crossing behaviour. The solid lines are fits obtained using a three coupled harmonic oscillator model yielding exciton–photon interaction strengths of 4.3 meV and 6.2 meV for the lh- and hh-excitons, respectively. The dashed lines correspond to the bare exciton frequencies and pure photonic crystal dispersion. Error bars correspond to the standard deviation of polariton energies. **b**, Mixing coefficients calculated using the coupled oscillator model show the photonic ($|\alpha|^2$), lh ($|\beta|^2$) and hh ($|\gamma|^2$) excitonic contribution to the upper, central and lower polariton branches (labelled UPB, CPB and LPB, respectively). At 35°, the CPB shows maximum mixing between the excitons and the photons and the coefficients are calculated to be $|\alpha|^2 = 0.4$, $|\beta|^2 = |\gamma|^2 = 0.3$.

Bragg dispersion. At smaller angles (35–45°), the low-frequency band edge strongly couples with the lh-excitonic lattice, resulting in the anti-crossing between these modes, along with the formation of the Bloch-lh-ELP bandgap. At even smaller angles (<35°), the low-frequency band edge of the modified bandgap interacts with the hh-excitonic lattice. This results in the formation of Bloch-lh-hh-ELPs with the associated anti-crossing and an additional propagation band inside a now further enhanced bandgap.

Although the theoretical estimates derived from experiments of the non-radiative lifetime (4.5 meV) and the interaction strength (4.3 meV) are comparable, the observation of anti-crossing and the formation of the propagation band confirm our assertion that we indeed have observed strong coupling between the excitonic lattice and photonic crystal Bloch modes.

An important advantage of the considered structures is the possibility to manipulate the optical properties by tuning the excitonic frequency, for instance, using an electric field. To enhance this property we designed our structures with a double-quantum-well basis, taking advantage of the enhanced quantum confined Stark effect in double-well structures[26]. In the presence of an electric field, excitonic resonances shift to longer wavelengths, thereby altering the interaction strength of the excitons and the Bloch modes, which also alter the reflectivity profile. We show the reflectivity spectra obtained by varying the electric field at three different angles in Fig. 5a, and the corresponding dispersion of these polaritons in Fig. 5b. As well as tuning the polariton contributions, we also observe a significant change in reflectivity (~100%). As these large changes in reflection can be induced by varying the electric field as well as the angle of incidence, this system can be useful for optical switching applications.

In summary, we demonstrate coherent interaction between low-frequency photonic crystal band edge photons and lh-excitons of the excitonic lattice. This is inferred from the significant reconstruction and enhancement of the reflection spectrum when the

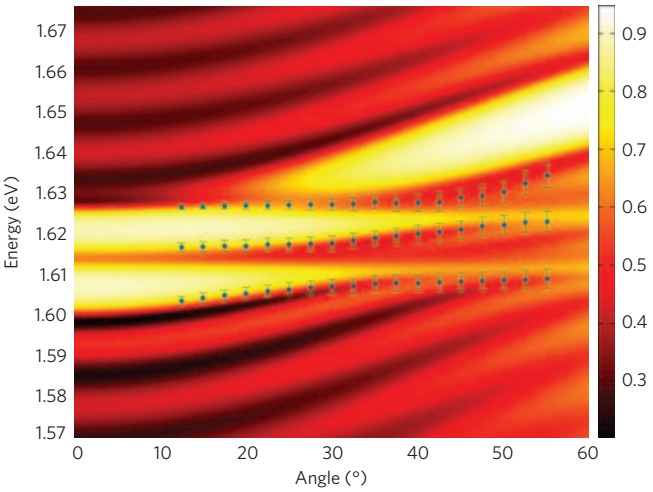

Figure 4 | Reflectivity simulations and experimental data. At large angles, when the photonic crystal bandgap is significantly detuned from the excitonic resonances, the band edges follow the expected Bragg dispersion. At smaller angles (35–45°), the low-frequency band edge strongly couples with the lh-excitonic lattice, resulting in the anti-crossing between these modes, along with the formation of the Bloch-lh-ELP bandgap. At even smaller angles (<35°), the low-frequency band edge of the modified bandgap interacts with the hh-excitonic lattice. This results in the formation of Bloch-lh-hh-ELPs with its associated anti-crossing and an additional propagation band inside a now further enhanced bandgap. The solid circles are the experimentally determined polariton dispersions, and the error bars correspond to the standard deviation of polariton energies.

stop-band of the underlying photonic crystal moves across the lh-excitonic frequency. A large enhancement of reflectivity is observed when the low-frequency edge of the Bloch-lh-ELP

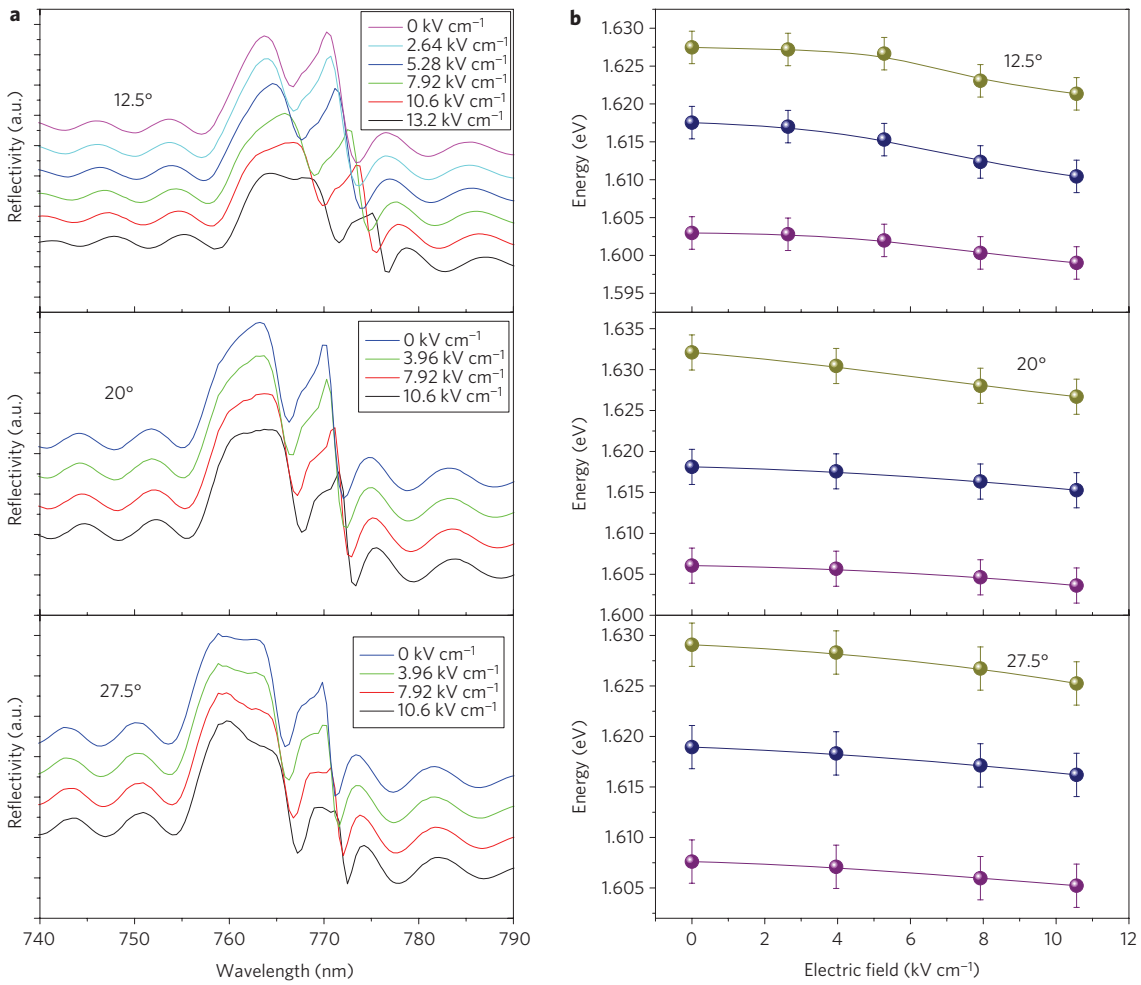

Figure 5 | Electric field tuning. a, Demonstration of polariton tuning using an electric field for reflectivity measurements at 12.5, 20, and 27.5°. At 12.5°, the top curve shows the reflection spectrum with no electric field. With increasing electric field (lower curves), we are able to manipulate the polaritonic nature of the central branch by decreasing its hh-excitonic component and increasing its photonic and lh-excitonic components. At 20°, a similar tunability is possible in which the hh-excitonic component becomes comparable to the photonic component. For a slightly greater angle of 27.5°, it is now possible to tune the contributions such that the two excitonic species play equal roles. In addition, large changes in reflectivity are observed. **b**, Dispersion of the three polariton branches as a function of electric field. The error bars correspond to the standard deviation of polariton energies.

bandgap crosses the hh-exciton frequency. This increase in reflectivity is accompanied by a dip between the lh- and hh-exciton frequencies. These effects are explained by coupling between hh-excitons and the Bloch-lh-ELP, which results in the formation of a new bandgap in the vicinity of the hh-excitons, and hybrid Bloch-lh-hh-ELP propagating excitations responsible for the dip in reflectivity. In addition, we show the tuning of the coherent interaction between the excitons and the Bloch modes of the photonic crystal using an electric field. This aspect of these polaritons can be used for slow-light enhanced nonlinear optics in such systems. Furthermore, the collective nature of the hybrid excitations demonstrated here opens up the possibility of observing macroscopic coherence phenomena in solid-state systems.

Methods

Structure details. The Bragg MQW sample studied in the present work was grown using solid-source molecular beam expitaxy and consisted of 70 periods of a double-quantum-well (DQW) basis consisting of 35 Å GaAs quantum wells separated by a 16 Å $Al_{0.22}Ga_{0.78}As$ barrier. This thin barrier causes the hybridization of excitons in the adjacent quantum wells, resulting in splitting of lh- and hh-excitons into two doublets[27,28]. Temperature-dependent photoluminescence measurements were carried out on a single DQW structure to identify the excitonic resonances.

In the Bragg structure, the DQWs are separated from each other by a 996 Å $Al_{0.22}Ga_{0.78}As$ layer. The concentration of aluminium in the barriers was chosen to create a structure with a non-negligible refractive index difference of 0.22, giving rise to the photonic-crystal aspect of the structure, while maintaining the contribution from the excitonic lattice introduced by the periodic arrangement of quantum wells.

Optical characterization. Measurements were carried out with the sample placed inside a temperature-controlled closed-cycle cryostat. A tungsten halogen lamp was used as the light source in the reflectivity measurements, and an argon ion laser (488 nm) was used as the excitation source in photoluminescence measurements. A charge-coupled device-based fibre coupled spectrometer was used to collect the optical signal in both the reflectivity and photoluminescence measurements.

Theory. We simulated the reflection spectra of our structure using the theoretical approach developed in ref. 14 based on non-local treatment of excitons, while taking into account modification of exciton–photon interaction due to refractive index contrast. The effects due to the refractive index contrast can be described by introducing an effective exciton susceptibility S, which has the form

$$S = \frac{\Gamma}{\omega - \omega_0 + i\gamma} + \Delta S(\omega) \quad (1)$$

where ω_0 and γ are the exciton frequency and non-radiative relaxation rate, respectively, ΔS reflects the presence of the refractive index contrast and is characterized by a non-singular frequency dependence, and Γ is the effective radiative decay rate of excitons, also modified by the refractive index contrast. The reflection coefficient for the structure with N periods is given by the formula

$$R_N = \left| \frac{S}{\cot(NKd)\sin(Kd) + i(S\cos\phi - \sin\phi)} \right|^2 \quad (2)$$

where K is the Bloch vector describing electromagnetic excitations of the structure, d is its period, and ϕ is the effective phase of excitations taking into account multiple reflection from the well–barrier interfaces[14]. As can be seen, the reflection spectrum is determined by the form of S and also the Bloch number K, the properties of which define the band structure of the system. In the frequency region of interest it is characterized by four band edges, which are solutions of the equation[15]

$$(\omega-\omega_0)(\omega-\Omega_+)\left[(\omega-\omega_0)(\omega-\Omega_-)-\frac{\Delta_\Gamma^2}{4}\right]=0 \qquad (3)$$

where Δ_Γ^2 is an effective coupling parameter proportional to Γ, and Ω_+ and Ω_- are the high- and low-frequency band edges of the pure photonic crystal, respectively. This equation describes coupling between the exciton and the low-frequency band edge state of the photonic crystal, while the high-frequency band edge state remains uncoupled. These band edges, two of which anti-cross under the strong coupling condition, form two photonic bandgaps separated by a propagation band.

The results of these calculations can also be used to interpret the Fano-like reflectivity spectra (Fig. 2b) in the vicinity of the hh-excitons, which interact with propagating Bloch modes of the photonic crystal rather than with band edge states. An approximate expression for reflectivity having a Fano form can be derived from equation (1) for the case where the exciton interacts with propagating modes of the photonic crystal given by

$$R_N \approx |R_{PC}|^2\frac{(\omega-\omega_0-\Gamma/\Delta S)^2+\gamma^2}{(\omega-\omega_0)^2+\gamma^2} \qquad (4)$$

where R_{PC} is the reflection coefficient of the corresponding photonic crystal structure. This expression is valid in the limit $R_{PC} \ll 1$, which is a reasonable assumption in the region of a propagating Bloch wave.

However, to explain the spectra in the region of coupled lh-hh excitation, the theory of ref. 14 should be modified to include the presence of the second excitons. This can be done by adding a second resonance term in the effective susceptibility of equation (1). This approach was used to simulate the reflectivity spectra in Fig. 4. We also fit the experimental data to a three coupled oscillator model. By doing so, we obtain values for the exciton parameter $\Gamma = 17.9$ μeV, corresponding to a coupling strength of 4.3 meV for the lh-excitons and $\Gamma = 37.5$ μeV for the hh-excitons, which corresponds to a 6.2 meV coupling strength.

Received 12 August 2009; accepted 25 September 2009; published online 25 October 2009

References

1. Dicke, R. H. Coherence in spontaneous radiation processes. *Phys. Rev.* **93,** 99–110 (1954).
2. Ivchenko, E. L., Nesvizhskii, A. I. & Jorda, S. Bragg reflection of light from quantum well structures. *Phys. Solid State* **36,** 1156–1161 (1994).
3. Deutsch, I. H., Spreeuw, R. J. C., Rolston, S. L. & Phillips, W. D. Photonic band gaps in optical lattices. *Phys. Rev. A* **52,** 1394–1410 (1995).
4. Hübner, M. *et al.* Optical lattices achieved by excitons in periodic quantum well structures. *Phys. Rev. Lett.* **83,** 2841–2844 (1999).
5. Inouye, S. *et al.* Superradiant Rayleigh scattering from a Bose–Einstein condensate. *Science* **285,** 571–574 (1999).
6. Scheibner, M. *et al.* Superradiance of quantum dots. *Nature Phys.* **3,** 106–110 (2007).
7. Deych, L. I. & Lisyansky, A. A. Polariton dispersion law in periodic-Bragg and near-Bragg multiple quantum well structures. *Phys. Rev. B* **62,** 4242–4244 (2000).
8. Sumioka, K., Nagahama, H. & Tsutsui, T. Strong coupling of exciton and photon modes in photonic crystal infiltrated with organic–inorganic layered perovskite. *Appl. Phys. Lett.* **78,** 1328–1330 (2001).
9. Birkl, G., Gatzke, M., Deutsch, I. H., Rolston, S. L. & Phillips, W. D. Bragg scattering from atoms in optical lattices. *Phys. Rev. Lett.* **75,** 2823–2826 (1995).
10. Ikawa, T. & Cho, K. Fate of the superradiant mode in a resonant Bragg reflector. *Phys. Rev. B* **66,** 085338 (2002).
11. Werchner, M. *et al.* One dimensional resonant Fibonacci quasicrystals: noncanonical linear and canonical nonlinear effects. *Opt. Express* **17,** 6813–6828 (2009).
12. Ivchenko, E. L. *et al.* Resonance optical spectroscopy of long-period quantum-well structures. *Phys. Solid State* **39,** 1852–1858 (1997).
13. Ivchenko, E. L., Voronov, M. M., Erementchouk, M. V., Deych, L. I. & Lisyansky, A. A. Multiple-quantum-well-based photonic crystals with simple and compound elementary supercells. *Phys. Rev. B* **70,** 195106 (2004).
14. Erementchouk, M. V., Deych, L. I. & Lisyansky, A. A. Optical properties of one-dimensional photonic crystals based on multiple-quantum-well structures. *Phys. Rev. B* **71,** 235335 (2005).
15. Erementchouk, M. V., Deych, L. I. & Lisyansky, A. A. Spectral properties of exciton polaritons in one-dimensional resonant photonic crystals. *Phys. Rev. B* **73,** 115321 (2006).
16. Biancalana, F., Mouchliadis, L., Creatore, C., Osborne, S. & Langbein, W. Microcavity polariton-like dispersion doublet in resonant Bragg gratings. Preprint at <http://arXiv:0904.0758v1> (2009).
17. Kavokin, A. V. & Kaliteevski, M. A. Light-absorption effect on Bragg interference in multilayer semiconductor heterostructures. *J. Appl. Phys.* **79,** 595–598 (1996).
18. Ammerlahn, D. *et al.* Influence of the dielectric environment on the radiative lifetime of quantum-well excitons. *Phys. Rev. B* **61,** 4801–4805 (2000).
19. Kasprzak, J. *et al.* Bose–Einstein condensation of exciton polaritons. *Nature* **443,** 409–414 (2006).
20. Amo, A. *et al.* Collective fluid dynamics of a polariton condensate in a semiconductor microcavity. *Nature* **457,** 291–296 (2009).
21. Gerace, D., Türeci, H. E., Imamoglu, A., Giovannetti, V. & Fazio, R. The quantum-optical Josephson interferometer. *Nature Phys.* **5,** 281–284 (2009).
22. Balili, R., Hartwell, V., Snoke, D., Pfeiffer, L. & West, K. Bose–Einstein condensation of microcavity polaritons in a trap. *Science* **316,** 1007–1010.
23. Saba, M. *et al.* High-temperature ultrafast polariton parametric amplification in semiconductor microcavities. *Nature* **414,** 731–735 (2001).
24. Lidzey, D. G., Bradley, D. D. C., Armitage, A., Walker, S. & Skolnick, M. S. Photon-mediated hybridization of Frenkel excitons in organic semiconductor microcavities. *Science* **288,** 1620–1623 (2000).
25. Erementchouk, M. V. *Dispersion Law of Exciton Polaritons in MQW Based Photonic Crystals*, vol. 5924, 59240R (SPIE, 2005).
26. Soubusta, J. *et al.* Excitonic photoluminescence in symmetric coupled double quantum wells subject to an external electric field. *Phys. Rev. B* **60,** 7740–7743 (1999).
27. Westgaard, T., Zhao, Q. X., Fimland, B. O., Johannessen, K. & Johnsen, L. Optical properties of excitons in $GaAs/Al_{0.3}Ga_{0.7}As$ symmetric double quantum wells. *Phys. Rev. B* **45,** 1784–1792 (1992).
28. Linnerud, I. & Chao, K. A. Exciton binding energies and oscillator strengths in a symmetric $Al_xGa_{1-x}As/GaAs$ double quantum well. *Phys. Rev. B* **49,** 8487–8490 (1994).

Acknowledgements

This work was supported by United States Air Force Office of Scientific Research (AFOSR) grant no. FA9550-07-1-0391.

Author contributions

All authors have contributed to this paper and agree to its contents.

Additional information

Reprints and permission information is available online at http://npg.nature.com/reprintsandpermissions/. Correspondence and requests for materials should be addressed to V.M.M.